Journal of Hydraulic Structures
J. Hydraul. Struct., 2024; 10(3): 51-71
DOI: 10.22055/jhs.2024.46835.1298

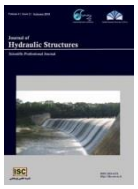

OPEN ACCESS

Application of machine learning methods on investigation the effect of interrupted deflector's height and downstream depth changes on energy dissipation at flip bucket spillways

Arash Adib[1]
Danial Ebrahimzadeh[2]
Mahmood Shafaei Bejestan[3]
Morteza Lotfirad[2]
Masoud Oulapour[2]

Abstract

Flip bucket is a type of energy dissipator structure. Flip buckets can sometimes be improved by adding wedge-shaped deflectors. This research introduced the best height proportion of used deflector on the flip buckets to increase energy dissipation. It used 4 types of deflector series including 32, 45, 47 and 55 degrees toward horizon with two different regular and irregular layouts and 19 different heights from 2.31 to 5.6 cm and in different hydraulic condition and the results were compared with a flip bucket without a deflector. The characteristics of laboratory flume were: length= 7.5 m, width= 0.58 m and height= 1.6 m. The results illustrates that the energy dissipation in the model with deflectors increased from 11.83 to 19.38 percent as compared with model without a deflector. The greatest percentage of energy dissipation was 80.74% which observed at a deflector angle of 55° and a discharge of 10 L/s, at deflector's ratio of n=0.8 and in non-uniform layout and in free hydraulic jump. Larger deflector angles and side lengths initially boosted energy dissipation, but this effect plateaued or even reversed at very large angles. For calculating energy dissipation and hydraulic jump length parameters, the regression relations were extracted in this research and results of this relations were compared with results of the gene expression programming (GEP), random forest (RF) and multivariate adaptive regression splines (MARS) methods. The results showed that the RF method is the most accurate method for calculating energy dissipation and hydraulic jump length parameters.

Keywords: Deflector, Flip bucket, Hydraulic jump, Froude number, RF

Received: 05 May 2024; Accepted: 26 May 2024

[1] Civil Engineering and Architecture Faculty, Shahid Chamran University of Ahvaz, Ahvaz, Iran, Email: arashadib@yahoo.com **(Corresponding author)**
[2] Civil Engineering and Architecture Faculty, Shahid Chamran University of Ahvaz, Ahvaz, Iran.
[3] Hydraulic Structure Department, Faculty of Water and Environmental Engineering, Shahid Chamran University of Ahvaz, Ahvaz, Iran.

1. Introduction

Without energy dissipaters, the powerful flow of water from a spillway can scour the riverbed downstream, eventually leading to structural problems and dam failure. These structures play a crucial role in safeguarding the dam and surrounding areas [1].

Because of the lack of appropriate design of an energy dissipation structure in spillways of dams, each year, many events have occurred in the world, these events endanger human lives, plants, animals, and the environment. The energy dissipation structures can reduce the number of these dangerous events and suitable design of these structures is an important problem. The flip buckets are one type of dissipating energy structure that is used to reduce the energy of the flow. The most common dissipators used in spillways are flip buckets, stepped chutes, and stilling basins with a hydraulic jump [2]. Depending on the geological and topographical features of the dam location, engineers often favor ski jump spillways with flip buckets as an economical way to handle water flow and energy reduction.

The following outcomes will be occurred because of ski-jump poor design [3]**:**

1- Bucket radius is too small Energy dissipation by dispersion may be insufficient

2- Extreme erosion due to water jet inopportune location to fall

3- Too small bucket trajectory angle makes energy dissipation by depreciation structure inadequate

Researchers [4] used a small-scale model to study how pressure distributes along a ski jump spillway equipped with a triangular flip bucket. These flip buckets are particularly useful in areas prone to cavitation, where water flow speeds exceed 15 to 20 meters per second [5]. Cavitation is the formation and collapse of bubbles which can damage the spillway structure. Flip buckets work by deflecting the high-speed water flow away from the dam itself. This reduces the risk of structural instability and erosion downstream [6]. In simpler terms, flip buckets act like a ramp, directing the forceful water flow away from the dam and protecting it from damage. Novak et al. [7] and Chadwick and Morfett [8] used diverse flip bucket types at the end of spillway and chutes. To achieve efficient energy dissipation, the flip bucket's minimum radius is recommended to be 3 to 5 times greater than the approaching flow depth. Additionally, the lip angle (or takeoff angle) should range from 20° to 35° to promote a jet spreading angle of roughly 5° in the air [9]. There are three parameters that they have a remarkable effect on the production of the maximum pressure and its magnitude: jet Froude number, relative bucket curvature, and the bucket angle [10]**.** Yamini et al. [11] conducted an experiment to analyze the influence of the entrance flow conditions on the pressure oscillations occurring on the bed of compound flip buckets. When there's more water coming in (higher depth and discharge) or the flow is less velocity (lower Froude number), the pressure on the spillway generally lessens. However, these conditions also lead to more frequent and larger variations in pressure (increased pressure fluctuations).

Nugroho et al. [12] surveyed the effect of the toothed spillway on the energy dissipation and the jump length with different arrangements and discovered that the length of hydraulic jump decreased compared to toothless mode and also energy dissipation soared about 30% to 50%. Deng et al. [13] presented a new type of ski-jump design and energy dissipation for baffled chute spillway. They analyzed the results and discovered that the optimal amount of the angular slope for desirable ski jump performance and sufficient amortization is from 30° to 45 °. Lian et al. [14] investigated the effect of the bucket type and angle on the downstream blade due to turbulent jet. Researchers compared the wind flow behind two types of spillway buckets (continuous and tab-shaped) at five different angles (40°, 45°, 50°, 55°, and 60°). They found that as the bucket angle increased, the height and width of the area affected by the downstream wind (think of it as the "wind blade") also increased. Interestingly, the effect on the length of the wind blade worked in

the opposite direction - it actually decreased with a larger bucket angle. The wind speed decreases in both types of buckets along the flow direction. Choi et al. [15] investigated the effect of deflector angle on the downstream grain of a submerged spillway. They tested four deflector models with angles of 0°, 30°, 45°, and 60° and discovered that the least angle for the deflector superior performance is 45° and in general a deflector can extend the throw length up to 40%. Daneshfaraz et al. [16] investigated how adding rough blocks to the base of an ogee spillway (a spillway with a particular curved shape) affects water flow. They looked at two aspects: how much energy is dissipated (lost) and how far the water travels (jet length). They tested spillways with and without a flip bucket (a structure at the end that redirects the water flow) at different angles. Their computer simulations showed the model accurately represented the water flow over the spillway. The presence of rough blocks on the spillway floor, in the absence of a flip bucket, resulted in a 15.4% increase in energy dissipation compared to a smooth floor configuration. When they added a flip bucket at 32 or 52 degrees, the increase in energy dissipation was slightly lower at 9.5%. In all cases, the rough blocks on the spillway floor significantly reduced the jet length by up to 58% compared to a smooth floor. Pourabdollah et al. [17] investigated how different types of stilling basins (structures used to control water flow) affect hydraulic jumps. They found that compared to a standard hydraulic jump, these basins resulted in a decrease in three key measurements: a) the depth of the calm water downstream (sequent depth) b) the depth of the turbulent flow within the jump (submerged depth) c) the total length of the zone where the jump occurs. The research by Heidarian et al. [18] centered on how the design of teeth (angle, arrangement, and radius) impacts three things: whirlpool formation, wasted kinetic energy, and the rate at which turbulence fades in the flow. The research revealed that unequal angles and a larger overall angle for the teeth were key factors in maximizing total turbulence loss. This implies that a strategic design with a mix of angles and a steeper tilt is most efficient in creating turbulence.

In addition to empirical studies, many types of research have been conducted using data mining techniques. A field of artificial intelligence that is related to representation and generalization using the data learning method is Machine learning (ML) [19].

Inspired by Darwin's theory of evolution, Gene Expression Programming (GEP) is a method that utilizes genetic operators like crossover and mutation to create improved solutions, similar to how new generations evolve in nature [20]. Several studies have compared GEP to other techniques for analyzing hydraulic phenomena. For example, researchers found GEP to be more accurate than methods like Support Vector Regression (SVR) and Artificial Neural Networks (ANN) when predicting characteristics of free hydraulic jumps in rough channels [21]. Similar results were obtained for studying hydraulic jumps in expanding channels and for determining discharge coefficients in ogee spillways [22 to 25]. These findings suggest that GEP is a powerful tool for analyzing hydraulic behavior, often surpassing traditional methods and other soft computing techniques [26].

Unlike most research on deflectors used with flip buckets, this study takes a fresh approach by analyzing how the angle and height of triangular deflectors on an ogee spillway affect both energy dissipation and the downstream hydraulic jump length. To understand how these deflectors work, researchers tested triangular deflectors of various sizes and angles under different water flow conditions. Using a technique called dimensional analysis, they were able to identify key factors (without specific numbers) that influence how much energy is dissipated and how long the hydraulic jump becomes with this type of deflector. Two relations to predicting energy dissipation and hydraulic jump length were obtained by multivariate nonlinear regression. Then, observed data were compared with results of different ML methods. The applied ML methods were GEP, RF and MARS methods. These methods have different bases. The base of GEP method is

nonlinear regression, evolutionary algorithm, the base of MARS method is linear nonparametric regression, and the base of RF method is ensemble learning under supervision and classification.

The research begins by highlighting the significance and need for the study.

Next, it delves into a technique called dimensional analysis, focusing on key hydraulic parameters.

The methodology section then details the materials and procedures used in the laboratory modeling stage.

Following that, the research explores the application of specific ML methods.

To analyze the findings, the next section utilizes graphs and laboratory observations.

Finally, the research culminates with a concluding section that summarizes the key takeaways.

In summary, the innovations and objectives of this research are:

- Simultaneous investigation of the effects of deflector height and angle on energy dissipation and hydraulic jump length downstream of a flip bucket. Two dimensionless relationships are derived for this purpose, whereas previous studies have not considered all of these factors.

- Selection of the best model among ML models that are prominent in water engineering (these models have different natures) for simulating energy dissipation and hydraulic jump length. Previous studies have typically used models with similar natures.

2. Material and methods

2.1. Dimensional analysis

Building a general correlation for flow energy dissipation begins with identifying the relevant variables that affect it. Ideally, these variables should be readily measurable input parameters to facilitate the development of a straightforward relationship. The energy dissipation of the flow over a flip bucket with a triangle deflector, ΔE, rely on the water density (ρ), the deflector angle (θ), the water dynamic viscosity (μ), the discharge per unit width of the approach channel (q), the bucket radius (R), the surface tension (σ), and the gravitational acceleration, (g), flow velocity (V), depth flow on the spillway (y), tailwater depth (y_t), opening ratio of the width of the flume ($\frac{\mathbf{L}}{\mathbf{B}}$), Reynolds number (Re), Weber number (We), the distance of the side deflectors to the channel wall (X_s), the distance of the deflectors from each other (X_m), height of the edge of the bucket from the floor of the channel (Z). These variables can be functionally expressed as:

$$\Delta E = f\ (\ \mu, \rho, \sigma, g\ ,V, R, Re\ ,We\ ,\ Fr\ ,\ \theta, \frac{y_t}{y}\ ,\ \frac{L}{B}, \frac{X_s}{X_m}, \frac{L_d}{L_b}) \quad (1)$$

Due to the turbulence of the flow in the present study and considering that the Reynolds number of the minimum flow is Re = 14171.6, so the ratio of viscosity to inertia is low and it has no effect on the motion of the flow, so we omit the Reynolds number in the effective parameters. Considering that the minimum height of water on the overflow crown in experiments is 2.8 cm (at a flow rate of 10 liters per second), the effects of surface tension and Weber number can be ignored [27].

We can express the relative energy dissipation (ΔE) of the flip bucket with a triangular deflector using a functional relationship that incorporates relevant parameters.

$$\Delta E = \frac{\Delta E}{E_0} = f\ (\mathrm{Fr}, \theta, \frac{y_t}{y}\ ,\ \frac{X_s}{X_m}, \frac{L}{B}, \frac{X_s}{X_m}, \frac{L_d}{L_b}) \quad (2)$$

$\frac{\mathbf{L}}{\mathbf{B}}$ = The opening ratio of the width of the flume, is equal to the transverse ratio of the flume that is not blocked by the deflectors to the total width of the flume, which is 0.35 in all experiments.

(Eliminated due to consistent value)

θ = The deflector angle to the horizon in terms of radians is equal to 0.558, 0.785, 0.82, 0.96.

$\frac{\mathbf{R}}{\mathbf{Z}}$ = The ratio of the radius of the bucket to the height of the edge of the bucket from the floor of the flume, which is constant in all experiments and is equal to 1.2 and does not help regression. (Eliminated due to fixed value)

$\frac{L_d}{L_b}$ = The ratio of the deflector length to the bucket chord length, which in all experiments has a constant value of 0.2. (Eliminated due to fixed value)

$\frac{X_s}{X_m}$ = The ratio of the distance of the side deflectors to the channel wall to the distance of the deflectors from each other, the value of this parameter is directly related to the arrangement of deflectors and in uniform and non-uniform arrangement is equal to 1 and 0.68, respectively. Utilizing a non-uniform arrangement mitigates the effects of the channel walls, leading to an increase in energy dissipation and a reduction in the length of the hydraulic jump downstream.

$\frac{\mathbf{y_t}}{\mathbf{y}}$ = The ratio of run-off depth to water depth at the overflow inlet. The value of y depends on the flow rate and the value of y_t is unique in each experiment.

Fr = The input Froude number to the cup which is a minimum of 6.331 and a maximum of 21.759.

2.2. Experimental model

Laboratory flume of hydraulic laboratory in the Water Sciences Faculty of Shahid Chamran University of Ahvaz was used as experimental model in this research. We used deflector series of four including 32, 45, 47, and 55 degrees toward the horizon with two different regular and irregular layouts. The heights of these deflectors are 2.31 to 5.6 cm based on 19 proportions from 0.33 to 0.8(the proportion was the height of the deflector to the critical depth of the maximum discharge). The layouts of deflectors were uniform and non-uniform layouts. The tests were performed by 12 discharges of 10 ,13.5 ,15 ,18 ,20 ,21 ,22 ,25 ,27 ,30, 32 and 35 Lit/s and three different tailwater conditions to create classical, semi-submerged and submerged hydraulic jumps. The total number of tests was 5508 tests. In all experiments, it was recorded the trajectory coordinate and all geometrical characteristics and hydraulic parameters before and after the ski jump. The features of flume and tests are:

Deflector design and testing:

- The deflectors were wedge-shaped with different angles and a width matching the flume channel (waterway). See Fig. 2 for examples.

-Researchers investigated deflectors with various angles (**θ=**32° to 55°) and a single size (L=10 cm side length).

-The deflectors were positioned at a specific height relative to the maximum water depth from the spillway (critical depth).

-The bottom of each deflector was kept parallel to the bottom of the flip bucket.

Experimental setup:

-A pump upstream of the channel-controlled water flow, measured by a flow meter.

-Water height over the spillway crest and the jet trajectory downstream were measured with a point gauge.

-Fig. 1 illustrates the overall setup (flip bucket, deflectors, etc.).

-Fig. 3 shows an example experiment with a specific flow rate and deflector angle.

Testing procedure:

-A total of 5508 tests were conducted with different flow rates, with and without deflectors.

-Key measurements throughout the tests included water discharge, tailwater depth, upstream and over-crest flow depths.

-Downstream flow depth was challenging to measure directly due to air bubbles and turbulence.

-To address this, a gate was used to create a hydraulic jump (a sudden increase in water depth) downstream, allowing for easier depth measurement.

-Using established relationships and the measured jump depth, researchers calculated the initial downstream depth.

-Finally, they calculated the energy dissipation of the water flow for each test using water depths and flow velocities upstream and downstream of the spillway.

Energy dissipation calculations:

-The calculations considered the energy before (upstream) and after (downstream) the flip bucket and the hydraulic jump.

-Specific formulas were used based on water depths and velocities at different points.

(a)

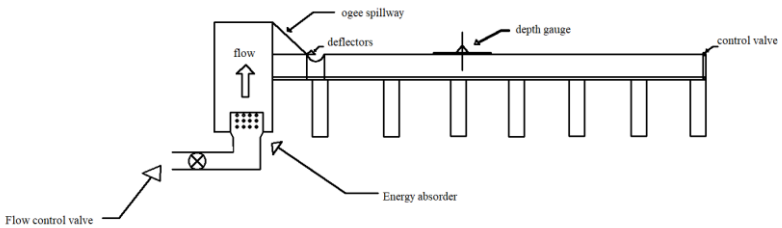

(b)

Figure 1. a) The used laboratory flume in this study b) A detailed cross-sectional view of the laboratory flume used in the experiment

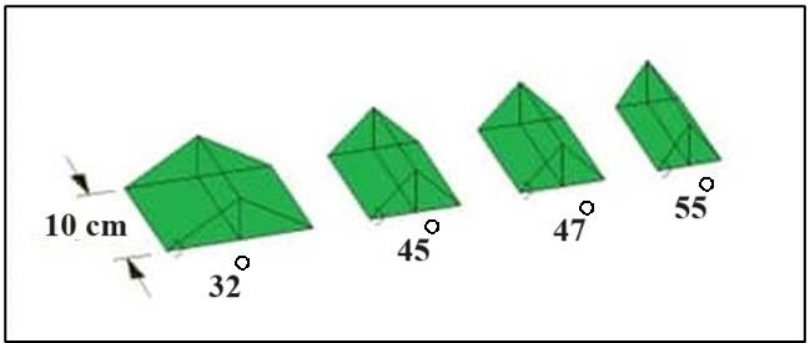

Figure 2. Geometric features of deflectors

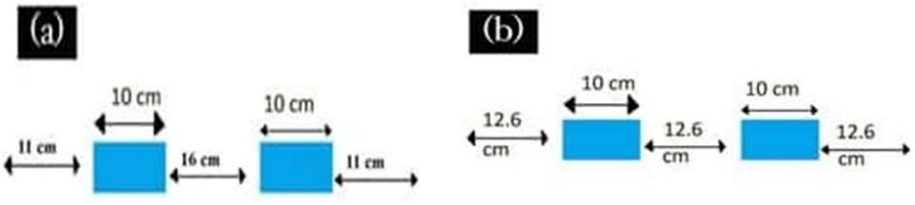

Figure 3. a) The position of the deflectors in non-uniform layout b) Uniform layout

Table 1. Parameters of the applied experimental models in this study

Deflector Characteristics	Flow Characteristics		
Θ	Q(L/s)		Tailwater conditions
Without a deflector	10	22	Classical hydraulic jump
32°	13.5	25	
45°	15	27	Semi-submerged hydraulic jump
47°	18	30	
55°	20	32	submerged hydraulic jump
	21	35	

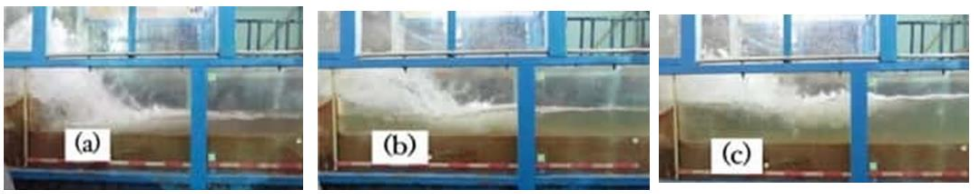

Figure 4. Experiment at the discharge of 15 L/s in the presence of a deflector with an angle of 32° in three different tailwater conditions: a) free b) semi-submerged c) submerged

In order to calculate the length of free hydraulic jump, the following experimental equation can be used:

$$L_j = A(y_2 - y_1) \quad (3)$$

A is an experimental coefficient whose value varies between 5 and 6.9 and for practical work it can be assumed to be equal to 6 [2].

Govinda Rao and Rajaratnam [28] to determine the length of submerged hydraulic jump presented a relationship:

$$L_j = [4.9(\frac{y_4 - y_2}{y_2}) + 6.1]\, y_2 \quad (4)$$

y_4 =Tailwater depth of Submerged hydraulic jump

y_2 =Tailwater depth of free hydraulic jump

Chow [29] showed that in rectangular channels with a horizontal floor, y_3 (initial depth of submerged jump) can be obtained from the following equation:

$$\frac{y_3}{y_4} = [1 + 2Fr_4^2(1 - \frac{y_4}{y_1})]^{\frac{1}{2}} \quad (5)$$

y_1 =Tailwater depth of free hydraulic jump

2.3. Conventional regression methods

The effectiveness of recommended ML models was assessed by comparing them to established methods like linear (LR) and non-linear regression (NLR). These traditional techniques were used to analyze the experimental data and derive equations describing both linear and non-linear relationships.

2.4. Gene Expression Programming (GEP)

In 2001, Ferreira [30] introduced Gene Expression Programming (GEP), inspired by Genetic Algorithms (GA) and Genetic Programming (GP). GEP offers several advantages. First, its genetic operators work directly on the chromosomes, leading to simpler diversity management. Second, GEP's unique multi-gene structure allows it to build complex applications with multiple subroutines.

Similar to GA, GEP uses biological evolution principles to create computer programs that simulate real-world phenomena [30]. GEP relies on two key elements: chromosomes, which contain the encoded genetic information, and expression trees, where this information is translated into functional programs [31]. Unlike GP, GEP uses simple, fixed-length chromosomes but allows for diverse tree structures to express the program logic.

The GEP algorithm stops when either a satisfactory solution is found or a predefined number of generations is reached [32]. The process starts by defining the function set (available operations), terminal set (data elements), a fitness function (to evaluate solutions), control parameters, and a stopping condition.

Initially, predicted values are compared to actual values. If the difference falls within a tolerance level, the process ends with the best solution found so far. Otherwise, chromosomes are selected for recombination (creating new variations) using a roulette wheel selection method. The fitness of these new chromosomes is then evaluated, and the cycle repeats until a satisfactory solution emerges [33].

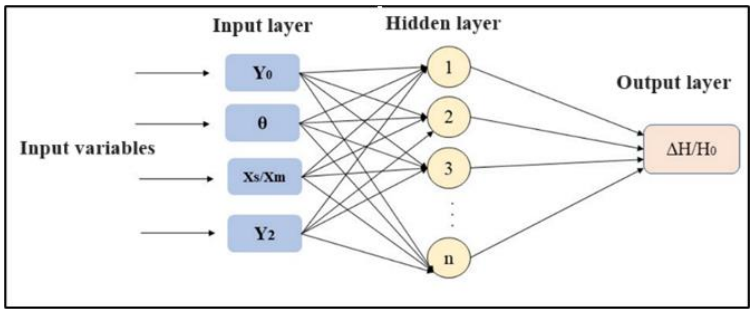

Figure 5. The specific design of the artificial neural network employed in this research

GEP utilizes traditional genetic operators alongside innovative techniques to achieve optimal solutions. The first step involves navigation, which creates an initial population of diverse candidate solutions encoded as chromosomes.

These chromos

omes are then translated into functional programs using a novel process called Expression Tree (ET). GEP uses fixed-length genes composed of terminals (representing variables like z1, z2, z3) and functional operators (+, ×, -, /, √, tanh, log, exp, etc.) [33,34]. Table 2 outlines the details of the GEP model. In this study, 70% of the data were used for training and 30% for testing.

Table 2. Details of the experimental models in this study

Parameter	Value
Number of Chromosomes	30
Head Size	7 and 8
Number of Genes	3
Linking Function	Addition
Fitness Function	MSE
Mutation Rate	0.039 & 0.042
Inversion Rate	0.1
One-Point Recombination	0.2
Two-Point Recombination	0.3
Gene Recombination	0.2
Gene Transposition	0.1
IS Transposition	0.1
RIS Transposition	0.1
Operator	+, - , ×, /, Pow, Sqrt, Exp, Ln, Atan, sin

2.5. Random Forest (RF)

The Random Forest algorithm is a supervised learning technique that leverages a group of decision trees to make predictions. As the name suggests, the forest is built randomly by combining multiple decision trees, often using a technique called bagging.

Bagging is a method that creates multiple decision trees from random data subsets. This helps to reduce the model's sensitivity to specific data points, resulting in a more stable and reliable final model.

Essentially, a Random Forest combines the strengths of several decision trees to make more robust predictions. It operates by constructing a set of regression trees based on a subset of training data. Three key parameters influence the forest's structure: the number of trees, the number of variables considered when splitting each node, and the maximum depth of the trees.

A significant advantage of Random Forests is that they do not require pruning the individual trees, which simplifies the modeling process. Additionally, they offer the versatility of handling both classification and regression tasks, making them a popular choice in ML applications [35].

Further details about the inner workings of Random Forests can be found in various research papers, such as the one by [36].

2.6. Multivariate Adaptive Regression Splines (MARS)

Developed by Friedman [37] in 1991, the MARS method excels at creating accurate models for various data types, including continuous, discrete, and binary variables. It's particularly adept at uncovering hidden patterns within the data.

The key to MARS's effectiveness lies in its unique structure, which combines three powerful approaches: standard linear regression, spline functions, and binary recursive partitioning.

-Linear Regression: MARS builds a foundation of linear regression models.

-Spline Functions: These functions introduce non-linearity by splitting the data into multiple regions with different linear relationships.

-Binary Recursive Partitioning: This technique systematically divides the data based on specific thresholds (called "knots") to create these different regions.

The resulting model combines multiple "basis functions" (BFs), each representing a linear relationship within a specific data region. Knots mark the boundaries between these regions. BFs are generated through a stepwise search process, ultimately leading to a flexible non-linear model.

$$Y = f(x) = \psi_0 + \sum_{m=1}^{M} \psi_m BF_m(x) \quad (6)$$

Y represents the outcome or dependent variable you're trying to predict.

BF stands for basis function, a building block of the model that captures a specific linear relationship within a data region.

x represents one or more predictor variables that influence the outcome (Y).

ψm denotes the coefficient associated with a particular basis function (BF). There can be multiple BFs (M total) in the final model, each with its own coefficient.

3. Results and discussion

In this study, firstly, with performing an experimental study and setting up free, semi-submerged and submerged hydraulic jumps, the data required to evaluate the performance of a new GEP model are examined and compared with the other researches. In the following, the results of prediction of free, semi-submerged and submerged hydraulic jumps characteristics by GEP model are presented. It should be mentioned that, in the present study, to ensure the free hydraulic jump formed exactly where the water jet struck the flume bottom, researchers strategically limited the water flow by partially closing the flume's exit valve. Also, in order to create semi- submerged and submerged hydraulic jumps in the first and second state, the valve to some extent was closed in proportion to the inlet flow of the water level downstream of the overflow, respectively, to the middle of the bucket and adjust its edge. It should be noted that the energy losses are due to the presence of the launcher structure (ogee spillway) has occurred alone, however, the energy losses have been solely due to the ski jump and the energy dissipation due to the downstream hydraulic

jump is not considered. As seen in the Fig. 6, in the control experiments as the flow rate decreases, the Froude number of inlet to the bucket increases, followed by this, the percentage relative energy losses have increased. These results clear that in high discharges, launcher structure's efficiency reduced, and energy dissipation of flip-bucket at high Froude numbers decreases and flip bucket has better efficiency in energy losses.

3.1. Energy dissipation

3.1.1. Experimental results

Fig. 7 compares the energy dissipation in different deflector angles(**θ**) used in this study. In general, it can be stated that the deflector angles 32°sand 45° have better performance in in energy dissipation as compared with other models. A maximum energy dissipation was about 80.74% which observed at a deflector angle of 55° and a discharge of 10 L/s, at deflector's ratio of n=0.8 and in non-uniform layout and in free hydraulic jump where the deflector's height was 5.6 cm. But Khalifehei et al. [6] showed that maximum energy dissipation was about 71% which observed at a deflector angle of 12° and a discharge of 10 L/s where the deflector's height was 0.6 cm. The minimum jump length was about 8.12%, which occurred at deflector angle of 47° and a discharge of 35 L/s, at deflector's ratio of n=0.33 and in uniform layout.

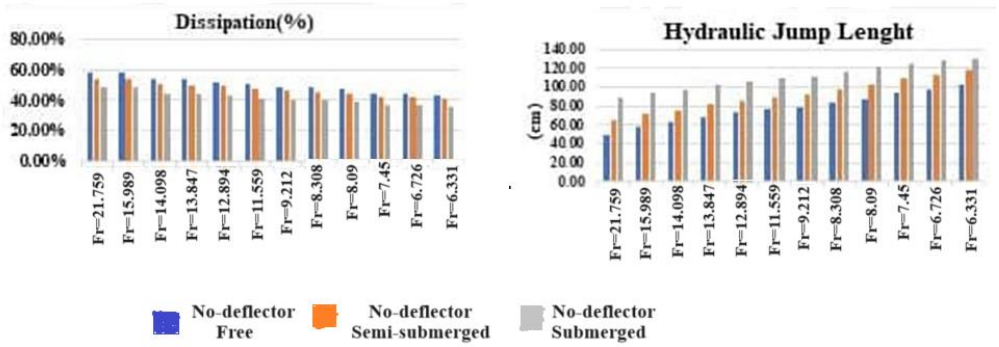

Figure 6. Control tests without deflector. A) Energy Dissipation, B) Hydraulic Jump Length

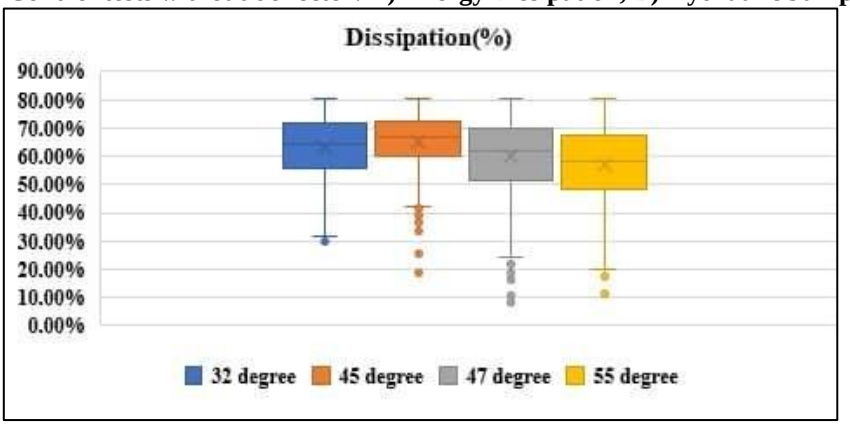

Figure 7. Energy dissipation in different deflector angles

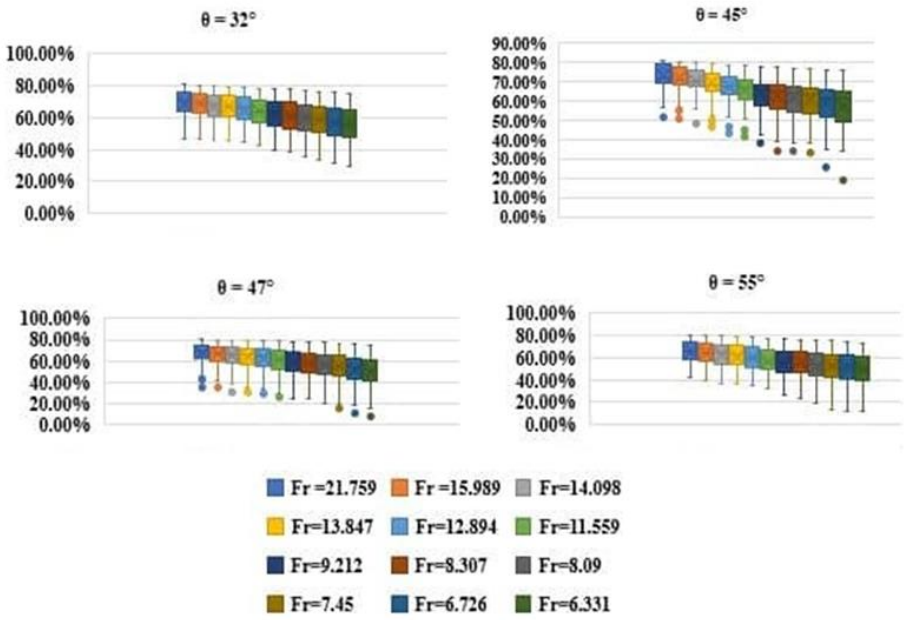

Figure 8. Percentage of energy dissipation in different deflector angle

Fig. 8 shows energy dissipation versus Froude number at different deflectors angles. As can be seen, energy dissipation decreases in all models, by decreasing the Froude number. Therefore, in a fixed angle model, Energy dissipation decreases with increase in discharge (yc). Comparing the results of the models with deflectors in Fig. 8 and without in Fig. 6 demonstrates that the bucket with a deflector causes higher energy dissipation than no- deflectors in all tests. It can be seen that in low Froude numbers (high discharges), the difference in energy dissipation versus no-deflector mode is less than in cases where the Froude number is higher, and this indicates that the arrangement of the deflectors in higher Froude numbers (lower discharge) that the inlet flow depth to the spillway is more effective.

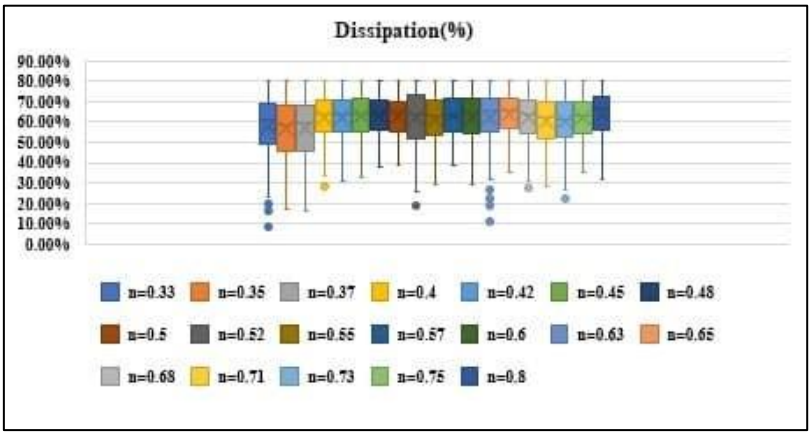

Figure 9. Percentage of Energy dissipation in different deflector's height ratios

Fig. 9 portrays the changes in the energy dissipation in all height deflector's ratios used in this study. Fig. 4 shows that the energy dissipation is steadily fluctuating as the ratio increases from

n=0.48 to n=0.57. The energy dissipation initially decreases with an increase in the deflector's height ratios from n=0.33 to n=0.54 and also from n=0.6 to n=0.8 which it experiences a downtrend at two larger ratios of n=0.33 and n=0.63. A maximum energy dissipation of about 80.74% was observed at a deflector angle of 55° and a discharge of 10 L/s, at deflector's ratio of n=0.8 and in non-uniform

layout, however, the minimum Energy dissipation was about 80.07%, which occurred at deflector angle of 47° and a discharge of 35 L/s, at deflector's ratio of n=0.33 and in uniform layout. Fig. 5 compares the Percentage of Energy dissipation in different deflector angles(θ) used in this study. Generally, we can conclude that the impact of the deflectors angle (**θ**) for a given deflector length, it can be stated that the deflector angles 45°sand 47° results in optimal energy dissipation as compared with the model without a deflector.

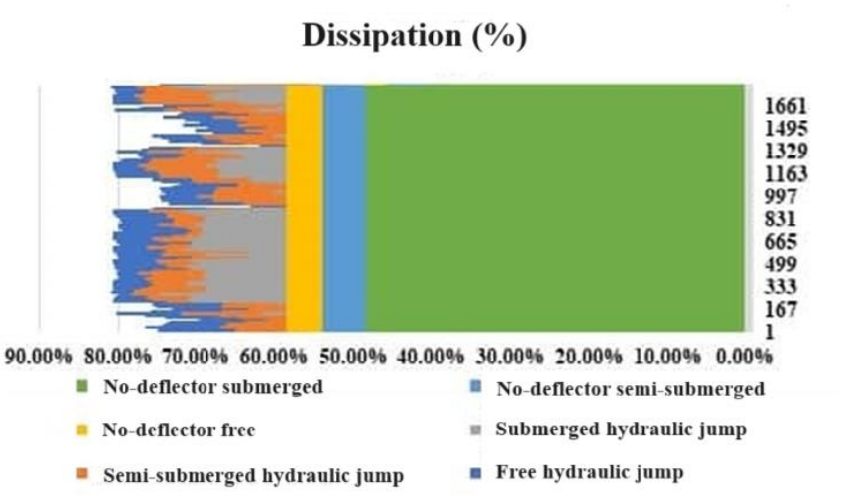

Figure 10. Energy dissipation in different condition

Fig. 10 shows energy dissipation in all different submergence condition. At a constant discharge with increasing downstream water depth, the percentage of relative energy loss decreases. Because with increasing the tailwater depth, the hydraulic jump at the downward moves towards the upward and the process of throwing the jet to downwards and depreciating due to ski jump does not occur completely. Jets are thrown from the flip bucket and deflectors before complete crossing through its curved path and depreciation due to collisions with air currents and each other to the tail water. So, in any definite discharge, the energy consumed by the flip bucket and deflectors in free hydraulic jump are more than 50% immersion ratio and energy dissipation in 50% immersion ratio is more than 100% immersion ratio

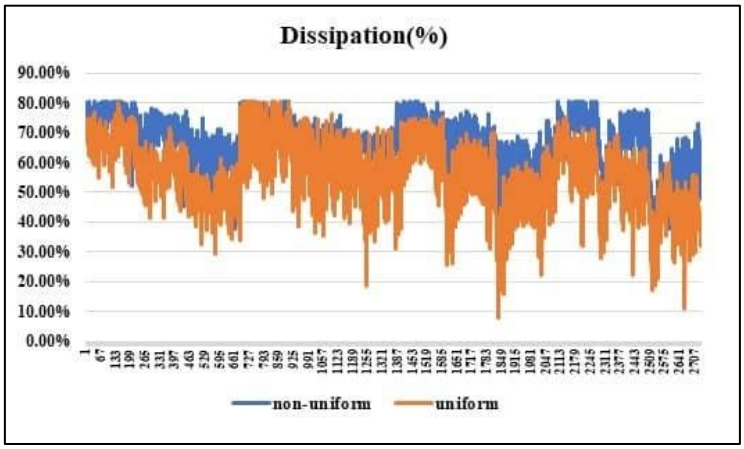

Figure 11. Energy dissipation in two different layouts

Fig. 11 portrays the energy dissipation in different layout condition. It's clear that in free, semi-submerged and submerged hydraulic jump modes in all Froude numbers, the non-uniform arrangement mode performed better than the uniform arrangement in energy dissipation and it was able to generate more depreciation. This performance has been such that the non-uniform arrangement has been able to create 17.1% more depreciation than the uniform arrangement. The reason for this difference is that in the non-uniform arrangement, the distance of the deflectors is less than the lateral arrangement of the side walls and the boundary layer formed between the overflow channel wall and the water flow causes more depreciation.

Eq. 7 was derived by multivariate nonlinear regression to predict energy dissipation in a flip bucket with a deflector, using the effective parameters extracted in the dimensional analysis section:

$$\boldsymbol{\Delta E} = \frac{-\mathbf{0.38}\left(log\frac{y_t}{y}\right)^{\mathbf{1.349}} + \left(\mathbf{0.454}\left(Fr_1^{\mathbf{0.194}}\right)\left(\frac{X_s}{X_m}\right)^{\mathbf{-0.25}}\right)}{\boldsymbol{\theta}^{\mathbf{0.096}}} \quad (7)$$

The statistical indices, R^2 and RMSE, were calculated to express the accuracy of the above correlations. R^2, RMSE for Eq. 7 were equal to 0.76 and 0.12 cm, respectively.

3.2. Jump length

3.2.1. Experimental results

Fig. 12 compares the hydraulic jump length in different deflector angles(θ) used in this study. In general, it can be stated that the deflector angles 32° and 47° results are optimal in hydraulic jump length as compared with other models. As can be seen in Fig. 6, generally, as Froude number got bigger, the jump length has decreased. It is obvious that the hydraulic jump length is steadily reducing as the Froude number increases from 6.331 to 21.759. A maximum jump length was about 259.4 cm which observed at a deflector angle of 45° and a discharge of 35 L/s, at deflector's ratio of n=0.8 and in uniform layout and submerged hydraulic jump, however, the minimum jump

length was about 0.98 cm which occurred at deflector angle of 32° and a discharge of 10 L/s, at deflector's ratio of n=0.48 and in non-uniform layout.

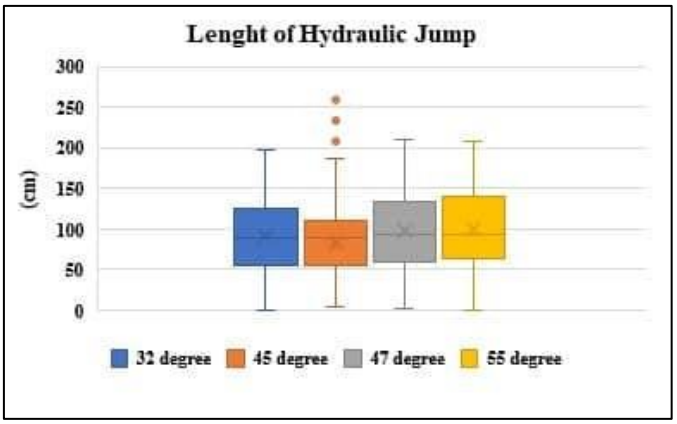

Figure 12. Length of Hydraulic Jump in different deflector angles(θ)

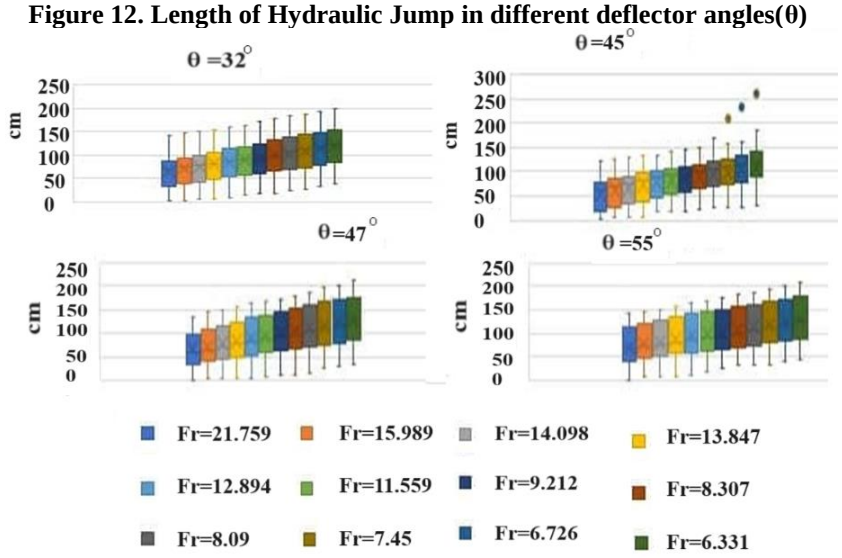

Figure 13. Length of Hydraulic Jump in deflector angle(θ)

Fig. 13 shows the hydraulic jump length against Froude number at different height ratios. Comparing the results of the models with deflectors in Fig. 13 and without in Fig. 6 represents that the bucket with a deflector affords reducing hydraulic jump length than example tests in some cases, while, in some ratios of deflectors used in this research, using deflectors has not any remarkable influence on the hydraulic jump length. As clearly seen in Fig. 14, the hydraulic jump length is steadily fluctuating as the ratio decrease from n=0.33 to n=0.52 in contrast, the hydraulic jump length initially increases with an increase in the deflector's height ratios from n=0.55 to n=0.8, however, it experiences a downtrend at two larger ratios of n=0.65 and n=0.8.

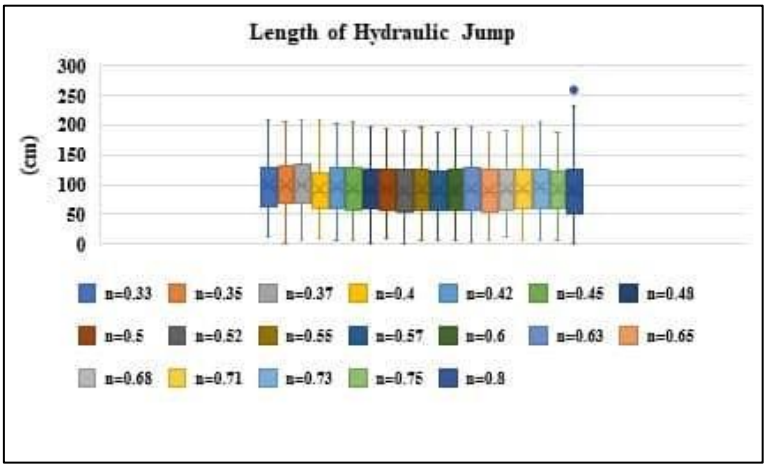

Figure 14. Length of Hydraulic Jump in different deflector's height ratios

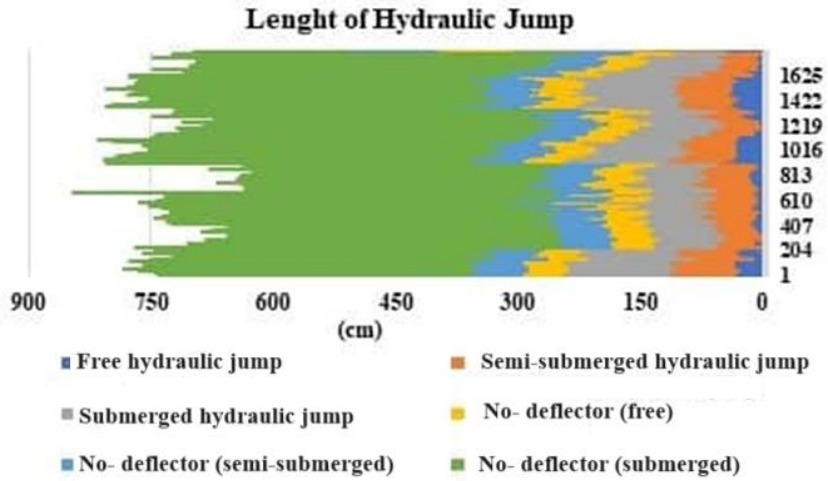

Figure 15. Hydraulic Jump Length in different submergence conditions

Fig. 15 shows the hydraulic jump length in two different submergence conditions. The results of measuring the length of the hydraulic jump downstream of the launcher structure indicate that in a certain flow rate, as the water depth downstream being less, the length of the hydraulic jump will be less. It means that in the adjusted mode downstream to form a free hydraulic jump, the free hydraulic jump length is less than the immersion ratio of 50% and in the 50% immersion ratio the jump length is shorter than the immersion ratio of 100%. In all Froude numbers increase in angle deflector from 32 to 45 degrees has reduced the length of the hydraulic jump and by increasing the angle deflector from 47 to 55 degrees we have seen an increase in the length of the hydraulic jump.

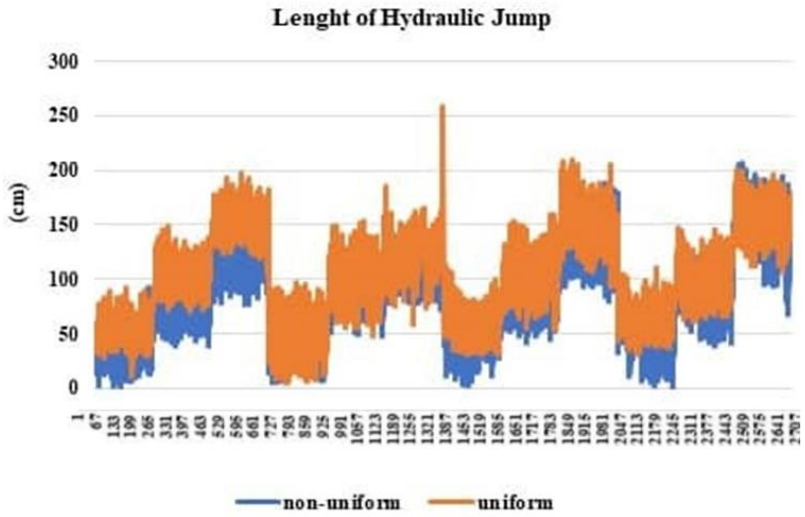

Figure 16. Hydraulic Jump Length in two different layouts

Fig. 16 illustrates the hydraulic jump length in two different layouts. It can be seen that in the free, semi-submerged and submerged hydraulic jump modes in all Froude numbers, the non-uniform arrangement mode performed better than the uniform arrangement in hydraulic jump length and was able to reduce length of hydraulic jump more. This performance has been such that the non-uniform arrangement has been able to reduce the hydraulic jump length 20.35% than the uniform arrangement.

Eq. 8 is the result of our analysis. We employed multivariate nonlinear regression, a statistical method, to create this equation. It predicts the hydraulic jump length in a flip bucket with a deflector, considering the important factors revealed earlier using dimensional analysis.

$$L_j = \frac{0.37\left(\frac{y_t}{y}\right)+\left(5.747\left(Fr_1^{-0.099}\right)\left(\frac{X_s}{X_m}\right)^{0.072}\right)}{\theta^{-0.014}} \quad (8)$$

To assess how well Eq. 8 predicts the actual jump length, we calculated two statistical measures: R^2 and RMSE. R^2 was 0.96, indicating a very good agreement between the predicted and measured values. RMSE was 18.61 cm, which means the equation's predictions typically differed from the real values by less than 19 cm.

The results of different ML methods are shown in Table 3 and Fig. 17 (Taylor diagram).

Table 3. Performance of utilized methods

Parameter	Period	Criteria	Reg	GEP	MARS	RF
ΔE	Training	R^2	0.76	0.75	0.77	0.85
ΔE	Test	R^2	0.70	0.70	0.75	0.86
ΔE	Training	RMSE (cm)	0.12	0.12	0.11	0.10
ΔE	Test	RMSE (cm)	0.14	0.13	0.11	0.09
Lj	Training	R^2	0.96	0.97	0.98	0.99
Lj	Test	R^2	0.90	0.90	0.96	0.98
Lj	Training	RMSE (cm)	18.6	18.50	18.10	17.98
Lj	Test	RMSE (cm)	19	19.2	18.2	18

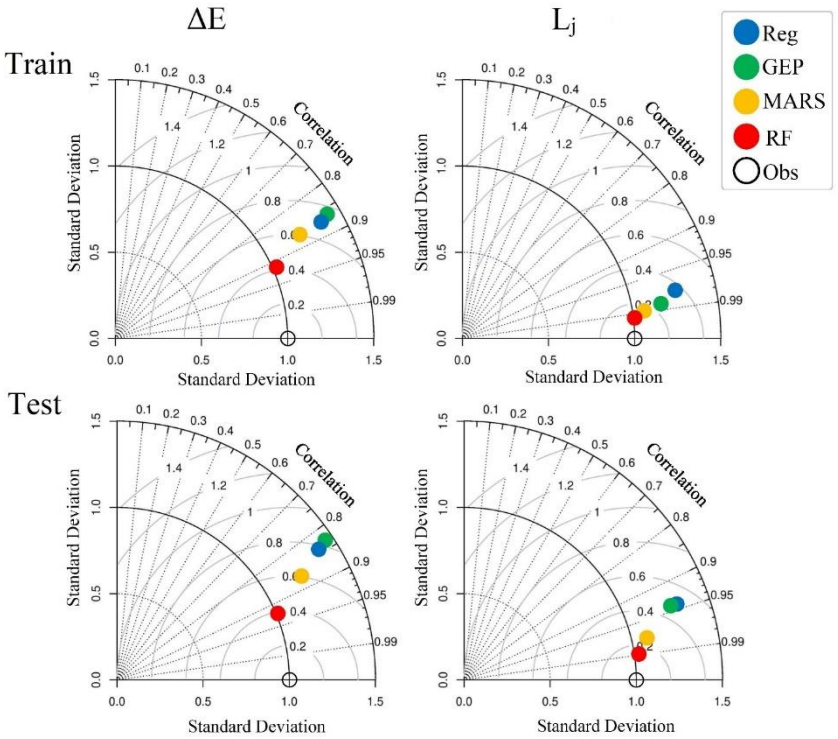

Figure 17. The Taylor diagram for the estimation of ΔE and Lj

Table 3 and the Taylor diagram illustrate that the RF model is the best method for estimating energy dissipation and hydraulic jump length. This method has the highest R^2 and the lowest RMSE. Among ML methods, the results of RF and MARS methods are more accurate than results of the extracted regression relations for energy dissipation and hydraulic jump length (Eqs. 7 and 8).

4. Conclusion

During the present study, the effect of the flip bucket besides the discontinuous transverse deflectors on the energy dissipation and hydraulic jump length surveyed. For this purpose, 5508 experiments including control and equipped with deflectors in four different angles and 19 different heights were performed, the summarizes of the results are given below. Overall, the addition of a triangular deflector to the flip bucket significantly improved its energy dissipation compared to models without one. This improvement was observed across different flow conditions: free, semi-submerged, and submerged hydraulic jumps. Specifically, the deflector increased energy dissipation by 19.5% (free jump), 14.63% (semi-submerged jump), and 11.8% (submerged jump) compared to the models without a deflector.

The study also found that the angle of the deflector (θ) plays a crucial role. As the angle increased, so did the energy dissipation, reaching an optimal range between 32° and 45°. Additionally, there seems to be a sweet spot for the deflector's height relative to the critical depth of the maximum discharge (n). The optimal height ratio was found to be n = 0.8.

Finally, this research achieved a significant outcome: a correlation for predicting the hydraulic jump length behind a flip bucket with a triangular deflector. This correlation was derived using dimensional analysis and multivariate nonlinear regression, considering the influence of multiple

factors. However, the results of measuring the length of the hydraulic jump at the downstream of ogee spillway indicates that in a certain flow rate, the lower water depth downstream, makes the hydraulic jump shorter. This means that in the downstream adjusted mode for free hydraulic jump, the hydraulic jump length is less than in the semi-submerged and in the semi-submerged, length of the hydraulic jump is shorter than the submerged hydraulic jump. An optimum angle of 32° was obtained with an optimal deflector's height ratio of n=0.52. Finally, we obtained a correlation by dimensional analysis and multivariate nonlinear regression for hydraulic jump length by a flip bucket with a triangular deflector.

In this study, four models with the nature of supervised ensemble learning (RF), nonparametric regression (MARS), evolutionary algorithm (GEP), and nonlinear regression were employed. The results of this study, with an R^2 of 0.99 in estimating the hydraulic jump length, are superior to the results obtained from the study by [21], which used the GEP model and reported an R^2 of 0.71. The results of this study are also significantly better than those of the study by [22], which estimated the R^2 of the jump length using the GEP model to be 0.7. Therefore, the use of ML models for estimating hydraulic parameters is highly accurate. Since these models do not require a lot of time to run, they are preferred over traditional methods for estimating hydraulic characteristics.

This study has some limitations that are recommended to be considered in future studies. These limitations include:

- The effect of deflector length on energy dissipation was not investigated.
- The phenomenon of cavitation at the deflector installation location was not investigated.
- Flip buckets with different geometries were not used, and the energy dissipation in them was not compared.

References

1. Arjenaki MO, Sanayei HRZ, (2020). Numerical investigation of energy dissipation rate in stepped spillways with lateral slopes using experimental model development approach. Model Earth Syst Environ 6(2): 605-616. https://doi.org/10.1007/s40808-020-00714-z
2. Hager W.H., Energy Dissipators and Hydraulic Jump. Water Science and Technology Library, vol 8. Springer, Dordrecht, pp.1-4,1992. https://doi.org/10.1007/978-94-015-8048-9_1
3. Vischer D.L., Hager W.H., Energy dissipators: IAHR hydraulic structures design manual 9. 1st Edition, Routledge, London, 208 p, 1995. https://doi.org/10.1201/9780203757512
4. Steiner R., Heller V., Hager W.H., Minor H.E., (2008). Deflector ski jump hydraulics. J Hydraul Eng 134(5): 562–571. https://doi.org/10.1061/ (ASCE)0733-9429(2008)134:5(562).
5. Khatsuria R.M., Hydraulics of spillways and energy dissipators. 1st Edition, CRC Press, Boca Raton, 680 p, 2004. https://doi.org/10.1201/9780203996980
6. Khalifehei K., Askari M.S., Azamathulla H., (2022). Experimental investigation of energy dissipation on flip buckets with triangular deflectors. ISH J Hydraul Eng 28(sup1): 292-298. https://doi.org/10.1080/09715010.2020.1775716
7. Novak P., Moffat A.I.B., Nalluri C., Narayanan R., Hydraulic structures. 4th Edition, CRC Press, London, 736 p, 2007. https://doi.org/10.1201/9781315274898
8. Chadwick A., Morfett J., Hydraulics in civil and environmental engineering. 1st Edition, CRC Press, London, 632 p, 2002. https://doi.org/10.4324/9780203027776
9. Mason P. (1984). Erosion of plunge pools downstream of dams due to the action of free-T-rajectory jets. P I Civil Eng 76(2): 523–537. doi:10.1680/iicep.1984.1257

10. Heller V., Hager W.H., Minor H.E., (2005). Ski jump hydraulics. J Hydraul Eng 131 (5): 347–355. doi:10.1061/(ASCE)0733-9429(2005)131:5(347)
11. Yamini O.A., Kavianpour M.R., Mousavi S.H., Movahedi A., Bavandpour M., (2018). Experimental investigation of pressure fluctuation on the bed of compound flip buckets. ISH J Hydraul Eng 24(1): 45–52. doi:10.1080/ 09715010.2017.1344572
12. Nugroho J., Soekarno I., Soeharno A.W.H., (2019). Experimental study of energy dissipation at baffled chute spillway. Jurnal Teknik Sipil, 26(1): 33-38. DOI: 10.5614/jts.2019.26.1.5
13. Deng J., Wei W., Tian Z., Zhang F., (2018). Design of a streamwise-lateral ski-jump flow discharge spillway. Water 10(11): 1585. https://doi.org/10.3390/w10111585
14. Lian J., He J., Gou W., Ran D., (2019). Effects of bucket type and angle on downstream nappe wind caused by a turbulent jet. Int J Env Res Pub He 16(8): 1360. https://doi.org/10.3390/ijerph16081360
15. Choi C.E., Ng C.W.W., Goodwin S.R., Liu L.H.D., Cheung W.W., (2016). Flume investigation of the influence of rigid barrier deflector angle on dry granular overflow mechanisms. Can Geotech J 53(10): 1751-1759. https://doi.org/10.1139/cgj-2015-0248
16. Daneshfaraz R., Ghaderi A., Akhtari A., Francesco S.D., (2020). On the effect of block roughness in ogee spillways with flip buckets. Fluids 5(4): 182. https://doi.org/10.3390/fluids5040182.
17. Pourabdollah N., Heidarpour M., Koupai J.A., (2020). Characteristics of free and submerged hydraulic jumps in different stilling basins. P I Civil Eng-Wat M 173(3): 121–131. https://doi.org/10.1680/jwama.19.00029
18. Heidarian P., Neyshabouri S.A.A.S., Khoshkonesh A., Bahmanpouri F., Nsom B., Eidi A., (2022). Numerical study of flow characteristics and energy dissipation over the slotted roller bucket system. Model Earth Syst Environ 8(4):5337-5351. https://doi.org/10.1007/s40808-022-01372-z
19. Sun M., Li Y., (2020). Eco-environment construction of English teaching using artificial intelligence under big data environment. IEEE Access 8: 193955–193965. doi: 10.1109/ACCESS.2020.3033068
20. Akhbari A., Ibrahim S., Zinatizadeh A.A., Bonakdari H., Ebtehaj I., Khozani Z.S., Vafaeifard M., Gharabaghi B., (2019). Evolutionary prediction of biohydrogen production by dark fermentation. Clean-Soil Air Water 47(1): 1700494. https://doi.org/10.1002/clen.201700494
21. Karbasi M., Azamathulla H.M., (2016). GEP to predict characteristics of a hydraulic jump over a rough bed. KSCE J Civ Eng 20(7): 3006–3011. https://doi.org/10.1007/s12205-016-0821-x
22. Roushangar K., Ghasempour R., (2018). Explicit prediction of expanding channels hydraulic jump characteristics using gene expression programming approach. Hydrol Res 49(3): 815–830. https://doi.org/10.2166/nh.2017.262
23. Salmasi F., (2021). Effect of downstream apron elevation and downstream submergence in discharge coefficient of ogee weir. ISH J Hydraul Eng 27(4): 375-384. https://doi.org/10.1080/09715010.2018.1556125
24. Nasrabadi M., Mehri Y., Ghassemi A., Omid M.H., (2021). Predicting submerged hydraulic jump characteristics using machine learning methods. Water Supply 21(8): 4180–4194. https://doi.org/10.2166/ws.2021.168
25. Bagatur T., Onen F., (2016). Computation of design coefficients in ogee-crested spillway structure using GEP and regression models. KSCE J Civ Eng 20(2): 951–959. https://doi.org/10.1007/s12205-015-0648-x

26. Samadi M., Sarkardeh H., Jabbari E., (2021). Prediction of the dynamic pressure distribution in hydraulic structures using soft computing methods. Soft Comput 25(5): 3873-3888. https://doi.org/10.1007/s00500-020-05413-6
27. ASCE (2000). Hydraulic modeling, Concepts and practice. Task Committee on Hydraulic Modeling, Environmental and Water Resources Institute, ASCE, Edited by R. Ettema, MOP 97. https://doi.org/10.1061/9780784404157
28. Govinda Rao N.S., Rajaratnam N., (1963). The Submerged Hydraulic Jump. J Hydraul Div, 89(HY1): 139-162. https://doi.org/10.1061/JYCEAJ.0000822
29. Chow V.T., Open Channel Hydraulics. McGraw-Hill, New York, U.S.A., 680 p, 1959.
30. Ferreira C. (2001). Gene expression programming: a new adaptive algorithm for solving problems. Complex Systems, 13(2): 87-129.
31. Ferreira C., Gene expression programming: mathematical modeling by an artificial intelligence. 2nd edition, Springer, Berlin, Germany, 480 p, 2006. https://doi.org/10.1007/3-540-32849-1
32. Bagherzadeh M., Mousavi F., Manafpour M., Mirzaee R., Hoseini K., (2022). Numerical simulation and application of soft computing in estimating vertical drop energy dissipation with horizontal serrated edge, Water Supply 22(4): 4676-4689. https://doi.org/10.2166/ws.2022.127.
33. Teodorescu L., Sherwood D., (2008). High energy physics event selection with gene expression programming. Comput Phys Commun 178(6): 409–419. https://doi.org/10.1016/j.cpc.2007.10.003
34. Kamari A., Sattari M., Mohammadi A.H., Ramjugernath D., (2016). Rapid method for the estimation of dew point pressures in gas condensate reservoirs. J Taiwan Inst Chem E 60: 258–266. https://doi.org/10.1016/j.jtice.2015.10.011
35. Breiman L., (2001). Random Forests. Mach Learn 45(1): 5–32. https://doi.org/10.1023/A:1010933404324
36. Lotfirad M., Esmaeili-Gisavandani H., Adib A., (2022). Drought monitoring and prediction using SPI, SPEI, and random forest model in various climates of Iran. J Water Clim Change 13(2): 383-406. https://doi.org/10.2166/wcc.2021.287
37. Friedman J.H., (1991). Multivariate adaptive regression splines. Ann Stat 19(1): 1-67. https://www.jstor.org/stable/2241837